Human Molecular Genetics, 2014, Vol. 23, No. 12 **3289–3298**
doi:10.1093/hmg/ddu042
Advance Access published on January 29, 2014

Adenylate cyclase 1 (*ADCY1*) mutations cause recessive hearing impairment in humans and defects in hair cell function and hearing in zebrafish

Regie Lyn P. Santos-Cortez[1], Kwanghyuk Lee[1], Arnaud P. Giese[3,4], Muhammad Ansar[1,5], Muhammad Amin-Ud-Din[6], Kira Rehn[4], Xin Wang[1], Abdul Aziz[5], Ilene Chiu[2], Raja Hussain Ali[5], Joshua D. Smith[7], University of Washington Center for Mendelian Genomics, Jay Shendure[7], Michael Bamshad[7], Deborah A. Nickerson[7], Zubair M. Ahmed[3], Wasim Ahmad[5], Saima Riazuddin[4] and Suzanne M. Leal[1,*]

[1]Department of Molecular and Human Genetics, Center for Statistical Genetics and [2]Bobby R. Alford Department of Otolaryngology—Head and Neck Surgery, Baylor College of Medicine, Houston, TX 77030, USA, [3]Division of Pediatric Ophthalmology and [4]Division of Pediatric Otolaryngology—Head and Neck Surgery, Cincinnati Children's Hospital Research Foundation, University of Cincinnati, Cincinnati, OH 45221, USA, [5]Department of Biochemistry, Faculty of Biological Sciences, Quaid-i-Azam University, Islamabad 45320, Pakistan, [6]Dera Ghazi Khan Campus, University of Education, Lahore 32200, Pakistan and [7]Department of Genome Sciences, University of Washington, Seattle, WA 98195, USA

Received October 16, 2013; Revised and Accepted January 27, 2014

Cyclic AMP (cAMP) production, which is important for mechanotransduction within the inner ear, is catalyzed by adenylate cyclases (AC). However, knowledge of the role of ACs in hearing is limited. Previously, a novel autosomal recessive non-syndromic hearing impairment locus DFNB44 was mapped to chromosome 7p14.1-q11.22 in a consanguineous family from Pakistan. Through whole-exome sequencing of DNA samples from hearing-impaired family members, a nonsense mutation c.3112C>T (p.Arg1038*) within adenylate cyclase 1 (*ADCY1*) was identified. This stop-gained mutation segregated with hearing impairment within the family and was not identified in ethnically matched controls or within variant databases. This mutation is predicted to cause the loss of 82 amino acids from the carboxyl tail, including highly conserved residues within the catalytic domain, plus a calmodulin-stimulation defect, both of which are expected to decrease enzymatic efficiency. Individuals who are homozygous for this mutation had symmetric, mild-to-moderate mixed hearing impairment. Zebrafish *adcy1b* morphants had no FM1-43 dye uptake and lacked startle response, indicating hair cell dysfunction and gross hearing impairment. In the mouse, *Adcy1* expression was observed throughout inner ear development and maturation. ADCY1 was localized to the cytoplasm of supporting cells and hair cells of the cochlea and vestibule and also to cochlear hair cell nuclei and stereocilia. *Ex vivo* studies in COS-7 cells suggest that the carboxyl tail of ADCY1 is essential for localization to actin-based microvilli. These results demonstrate that ADCY1 has an evolutionarily conserved role in hearing and that cAMP signaling is important to hair cell function within the inner ear.

* To whom correspondence should be addressed at: Department of Molecular and Human Genetics, Center for Statistical Genetics, Baylor College of Medicine, 1 Baylor Plaza 700D, Houston, TX 77030, USA. Tel: +1 7137984011; Fax: +1 7137984012; Email: sleal@bcm.edu

INTRODUCTION

One in 1000 children is born with hearing impairment, but only ~60% have a family history of hearing impairment or a confirmed genetic etiology and >80% do not have syndromic features (1). Non-syndromic hearing impairment is highly heterogeneous: ~170 loci have been mapped across the genome and causal mutations in close to 80 genes have been identified (Hereditary Hearing Loss Homepage, http://hereditaryhearingloss.org). It is expected that hundreds of genes that harbor mutations that are causal for hearing impairment are yet to be identified.

Previously, an autosomal recessive non-syndromic hearing impairment locus, DFNB44, was mapped in a consanguineous family 4009, which is a Siraki-speaking kindred from a remote rural village in Punjab province, Pakistan. DFNB44 was mapped to chromosome 7p14.1-q11.22 with a statistically significant maximum multipoint LOD score of 5.0 (2). Both the 3-unit support interval and the region of homozygosity included a 31.5 Mb locus (chr7:37.56–69.07 Mb) that contains 167 genes. In the original DFNB44 report (2), family 4009 (Fig. 1A, Branch 1) included five hearing-impaired individuals from two second-cousin marriages. Since then, three hearing-impaired and three unaffected individuals have also been ascertained (Fig. 1A, Branch 2). DNA samples from individuals in branch 2 also underwent a whole genome scan using 388 short tandem repeat (STR) markers. Here, we report the identification of a mutation within *ADCY1* (MIM 103072), which encodes adenylate cyclase 1, as the cause of hearing impairment within the two branches of this family.

RESULTS

The affected family members of family 4009 have pre-lingual hearing impairment, use sign language for communication and can only speak a few basic words but speech is unclear and is understandable only to immediate family members. Unlike their relatives with normal hearing, hearing-impaired individuals were not able to go to school. The family did not report any history of ear discharge or neurologic and systemic symptoms. No other risk factors were identified as a possible cause of hearing impairment. Upon physical examination, no signs of intellectual disability, gait disorders or vertigo were identified.

Six of the eight individuals with hearing impairment, namely V-7, VI-3, VI-4, VI-5, VI-7 and VI-8, underwent standard audiometric testing (Fig. 1B, Supplementary Material, Fig. S1). Five of these individuals demonstrated bilateral symmetric mild-to-moderate hearing impairment, while individual VI-7 had asymmetric impairment with profound loss in the worse ear. Noticeably individual VI-7 had an air-bone gap of at least 30 dB at mid-to-high frequencies in the left ear, whereas the right ear had predominantly moderate-to-severe sensorineural impairment, suggesting a middle ear problem mainly in the left ear (Supplementary Material, Fig. S1). Additionally, five of the six individuals tested had mixed hearing impairment, while individual VI-8 had moderate conductive hearing impairment based on unmasked thresholds despite an air-bone gap of >50 dB at the low frequencies (Supplementary Material, Fig. S1). Median threshold values from all audiograms indicated mild sensorineural hearing impairment at 2–4 kHz and moderate mixed impairment at the low frequencies (Fig. 1B). Furthermore, a dip in threshold can be found in all audiograms at 6–8 kHz (Fig. 1B). These results indicate that the mutation of *ADCY1* affects inner ear function at all frequencies, with worse affectation at low and high frequencies.

One hearing-impaired individual per family branch was selected for whole-exome sequencing (WES) because it was thought that different variants could be segregating with hearing impairment in each branch based on genome scan haplotype information and additionally the two branches were reported to be related only by marriage. DNA samples from individuals VI-3 from Branch 1 and V-9 from Branch 2 (Fig. 1A) were submitted for WES. These two individuals were selected for WES because, based on genome scan data, individual VI-3 was homozygous for the DFNB44 haplotype while individual V-9 did not carry the same DFNB44 haplotype (Fig. 1A). An additional consideration for the selection of individuals for WES was sufficient availability of DNA. For WES variants that were homozygous for the non-reference allele, potentially functional variants including nonsense, missense, splice site and indels were screened against public variant databases dbSNP (http://www.ncbi.nlm.nih.gov/projects/SNP), 1000 Genomes (http://www.1000genomes.org) and Exome Variant Server (http://evs.gs.washington.edu/EVS/). When the two individuals were analyzed separately for homozygous variants across the genome that passed all quality control measures and that were also not found in variant databases, a total of 21 variants were identified for individual VI-3, of which 4 were predicted to be damaging, while for individual V-9, 27 variants were identified of which 5 were predicted to be damaging (Supplementary Material, Table S1). Only two rare variants, a missense variant within *HECW1* (MIM 610384, NM_015052.3) c.2195T>C (p.Val732Ala) and a nonsense variant c.3112C>T (p.Arg1038*) within *ADCY1* (NM_021116.2), were found to be homozygous in both individuals (Supplementary Material, Table S2). These variants both lay within the DFNB44 interval. The *HECW1* missense variant is most likely benign and was predicted to be damaging by only one out of six prediction algorithms (3–9). DNA samples from all 4009 family members were Sanger-sequenced for both the *ADCY1* and *HECW1* variants, but only the *ADCY1* variant segregates with hearing impairment (Fig. 1A and C). Additionally, the *ADCY1* c.3112C>T (p.Arg1038*) variant was not identified in 650 ethnically matched control chromosomes.

Parametric linkage analysis was performed using the *ADCY1* variant genotypes and resulted in a two-point LOD score of 5.8 at $\theta = 0$. Although individuals VI-3 and V-9 do not share a homozygous haplotype based on STR markers, from genotypes obtained from WES these two individuals share a common homozygous haplotype surrounding *ADCY1*: individual VI-3 is homozygous for all variants within the chr7:38.31–72.21 Mb region and individual V-9 is homozygous for all variants within the chr7:42.09–47.32 Mb region. The shared region of homozygosity includes 80 variant sites and 20 of these variant sites are homozygous for the minor allele (Supplementary Material, Table S2). All variants within the region of homozygosity were observed in variant databases with the exception of the *HECW1* and *ADCY1* variants.

The ADCY1 p.Arg1038* variant is predicted to be deleterious by PROVEAN (http://provean.jcvi.org/index.php; 4), MutationTaster (http://www.mutationtaster.org; 6) and LRT (http://www.genetics.wustl.edu/jflab/; 8). The stop-gained mutation is

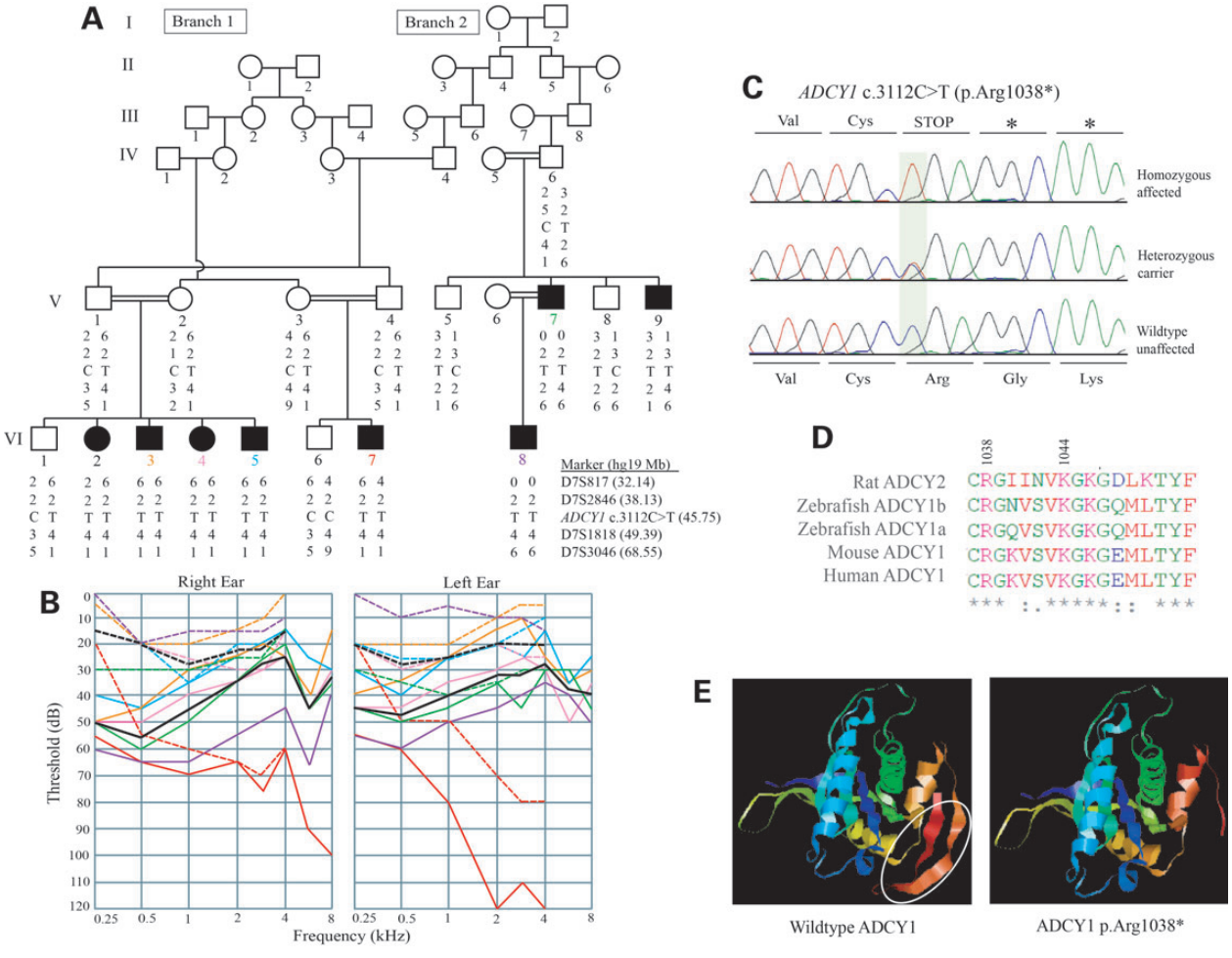

Figure 1. Pedigree, mutation and audiogram data. (**A**) Family 4009 with the c.3112C>T (p.Arg1038*) mutation segregating with hearing impairment. (**B**) Audiogram information from six hearing-impaired individuals from family 4009. *Colors* for the individual's ID number in (A) match the line colors for each audiogram. Solid lines, air conduction; broken lines, bone conduction; black lines, median values per frequency. (**C**) Chromatograms comparing a hearing-impaired individual who is homozygous for the *ADCY1* variant, a heterozygous carrier and a control individual. (**D**) Alignment of amino acids 1037–1053 of human ADCY1 with mouse ADCY1, zebrafish ADCY1a and ADCY1b and rat ADCY2. The arginine residue at 1038 and the lysine residue at 1044 are labeled and are identical in the aligned sequences. (**E**) Molecular modeling of wild-type and truncated ADCY1, which shows loss of two terminal β sheets (encircled) due to the p.Arg1038* variant.

also predicted to remove 82 amino acids that form two β sheets of the cytoplasmic carboxyl tail (Fig. 1C and E) and include highly conserved residues at the C_2 domain (Fig. 1D, Supplementary Material, Fig. S2). The sequences of 9 human ADCY proteins and 52 non-human ADCY1 proteins were aligned. The multiple sequence alignment revealed a highly conserved motif that corresponds to positions 1037–1053 of ADCY1 (Fig. 1D, Supplementary Material, Fig. S2). Furthermore, the conserved segment is ∼60% similar among human adenylate cyclase (AC) proteins, while this motif in ADCY1 is >80% similar to those within the ADCY5 and ADCY6 sequences (Supplementary Material, Fig. S2B). The same sequence motif that is highly conserved across species is also conserved in nine human AC proteins (Fig. 1D, Supplementary Material, Fig. S2).

To determine whether *ADCY1* has an evolutionarily conserved role in hearing, hair cell function via *adcy1* was tested in the zebrafish model. Due to similarity in the morphology and function of the inner ear and lateral line hair cells of zebrafish to vertebrate inner ear hair cells, the zebrafish has been used in the identification of inner ear-expressed genes that are evolutionarily conserved and in which mutations cause hearing defects in mice and humans (10,11). The zebrafish has two copies of *adcy1*, namely *adcy1a* (NM_001168349) and *adcy1b* (NM_001168350), the protein products of which are both 72% identical and 82% similar to human ADCY1. Previously, *adcy1a* and *adcy1b* morphants have been described, but only for expression in retinal ganglion cells and for misprojection of retinal axons (12) and not for hearing loss. For this study, gene-copy-specific zebrafish morphants were generated and tested for hearing and hair cell function. Both *adcy1a* and *adcy1b* zebrafish have obvious morphological defects, including axis curvature and reduced eye and brain size (Fig. 2A), which are more severe in *adcy1a* morphants (Supplementary Material, Fig. S3). While almost all the *adcy1a* morphants responded to acoustic stimuli, <5% of the *adcy1b* morphants responded (Fig. 2B). These observations suggest that *adcy1b* but not *adcy1a* is essential for hearing in zebrafish. Despite the occurrence

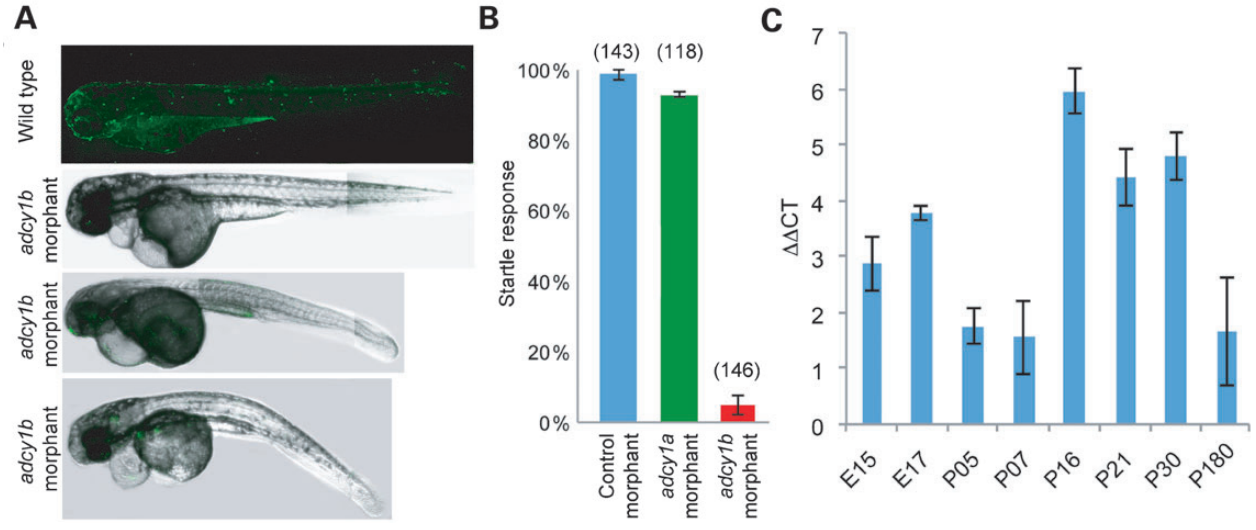

Figure 2. Hearing deficit from suppression of *adcy1b* expression in zebrafish embryos and *ADCY1* expression in mouse inner ear. (**A**) Comparison of FM1-43 labeling in larvae with various developmental defects showed the absence or marked reduction of uptake in *adcy1b* morphants, while the *adcy1a* morphants had normal FM1-43 dye uptake (Supplementary Material, Fig. S3). (**B**) Acoustic startle reflex of 5-day-old *adcy1a* and *adcy1b* morphants along with control morpholino-injected embryos. In contrast to wild-type and *adcy1a* morphants, a significant percentage of *adcy1b* morpholino-injected larvae did not respond to acoustic stimuli, indicating hearing impairment. Data are shown as mean ± SEM. (**C**) Real-time PCR analysis of the *Adcy1* mRNA level in C57BL/6J mouse temporal bones at eight different developmental stages. C_T is the observed threshold number of PCR cycles required for detection of the amplification product. ΔC_T is the calculated difference in C_T between *Adcy1* and an internal control standard (*Gapdh*) measured in the same sample. $\Delta\Delta C_T$ is the calculated difference in ΔC_T between the experimental and P3 time points. Real-time PCR was performed in triplicates and was repeated twice ($n = 6$).

of severe developmental defects, the *adcy1a* morphant had normal uptake of FM1−43 (Supplementary Material, Fig. S3), a styryl pyridinium dye that enters the hair cells via mechanotransduction (MET) channels in a Ca^{2+}-calmodulin-dependent manner (13). On the other hand, *adcy1b* morphants had very few or no fluorescent neuromast at 72 h post-fertilization (Fig. 2A), which could be due to non-functional or degenerating MET components in lateral line hair cells.

Gene expression and ADCY1 localization were also tested in inner ears of the mouse and rat. *Adcy1* is present throughout the development and maturation of mouse inner ear, with the highest expression at P16 (Fig. 2C). Furthermore, mRNAseq transcriptome data showed an ∼1.5-fold enrichment of *Adcy1* mRNA in mouse cochlear hair cells at P0 compared with supporting cells (Shared Harvard Inner-Ear Laboratory Database, https://shield.hms.harvard.edu). Immunoreactivity was found in the sensory epithelia of both cochlear and vestibular tissues (Fig. 3). In the organ of Corti, ADCY1 immunoreactivity was more prominent in inner hair cells and pillar cells. However, ADCY1 was also present in the outer hair cells and, to a lesser extent, in supporting cells surrounding outer hair cells (Fig. 3). In cochlear hair cells, ADCY1 immunofluorescence was distributed throughout the cell body and nuclei (Fig. 3B and F), and there was a barely detectable level in stereocilia (data not shown). In contrast, ADCY1 was found throughout the cytoplasm of sensory epithelium of vestibular end organs, but was not observed in the nuclei or hair cell bundles (Fig. 3J and N). No specific immunoreactivity was observed when the primary antibody was omitted.

As rat cochlear hair cells have longer stereocilia (14), we immunostained the adult organ of Corti and vestibular tissues in the rat (Fig. 4) to better characterize the expression in the stereocilia at high resolution. Similar to the mouse, ADCY1 was localized to hair cells and supporting cells in the rat organ of Corti and vestibular tissue (data not shown). In the rat cochlea, weak ADCY1 immunoreactivity was observed in the stereocilia and cuticular plate of hair cells (Fig. 4). ADCY1 was detected along the length of both the outer and inner hair cell stereocilia (Fig. 4E and H). However, like mouse tissue, no prominent hair bundle labeling was observed in the utricular sensory cells (Fig. 4K). These observations suggest a unique role for ADCY1 in cochlear hair cell stereocilia and may reflect the functional or structural differences between cochlear and vestibular hair bundles.

COS-7 cells contain actin-rich microvilli at the cell surface and have been used as *in vitro* models to examine F-actin and protein dynamics (15). To determine the mechanism and the effect of the ADCY1 p.Arg1038* variant, COS-7 cells were co-transfected with GFP-tagged human *ADCY1* constructs. We observed a significant enrichment of ADCY1-GFP in the apical (microvillar) and lateral plasma membrane 24 h following transfection (Fig. 5A). We also observed the expression of ADCY1-GFP in the cytosol of transfected cells (Fig. 5A). Identical results were observed with tdTomato-tagged ESPN and GFP-tagged wild-type ADCY1 (Supplementary Material, Fig. S4C). In contrast to wild-type protein, the p.Arg1038* variant yielded a protein that displayed no labeling in the cell membrane and microvilli of transfected COS-7 cells (Fig. 5A). Additionally, the protein appeared to be diffusely located throughout the cytoplasm, with weak nuclear labeling (Fig. 5A). To find out if the p.Arg1038* variant alters the stability of ADCY1, we probed western blot containing the protein extracts derived from COS-7 cells transiently expressing wild-type and p.Arg1038* mutant constructs. No statistically significant reduction in amount of mutant protein was observed when compared with wild-type ADCY1 (Fig. 5B). Taken together with our high-

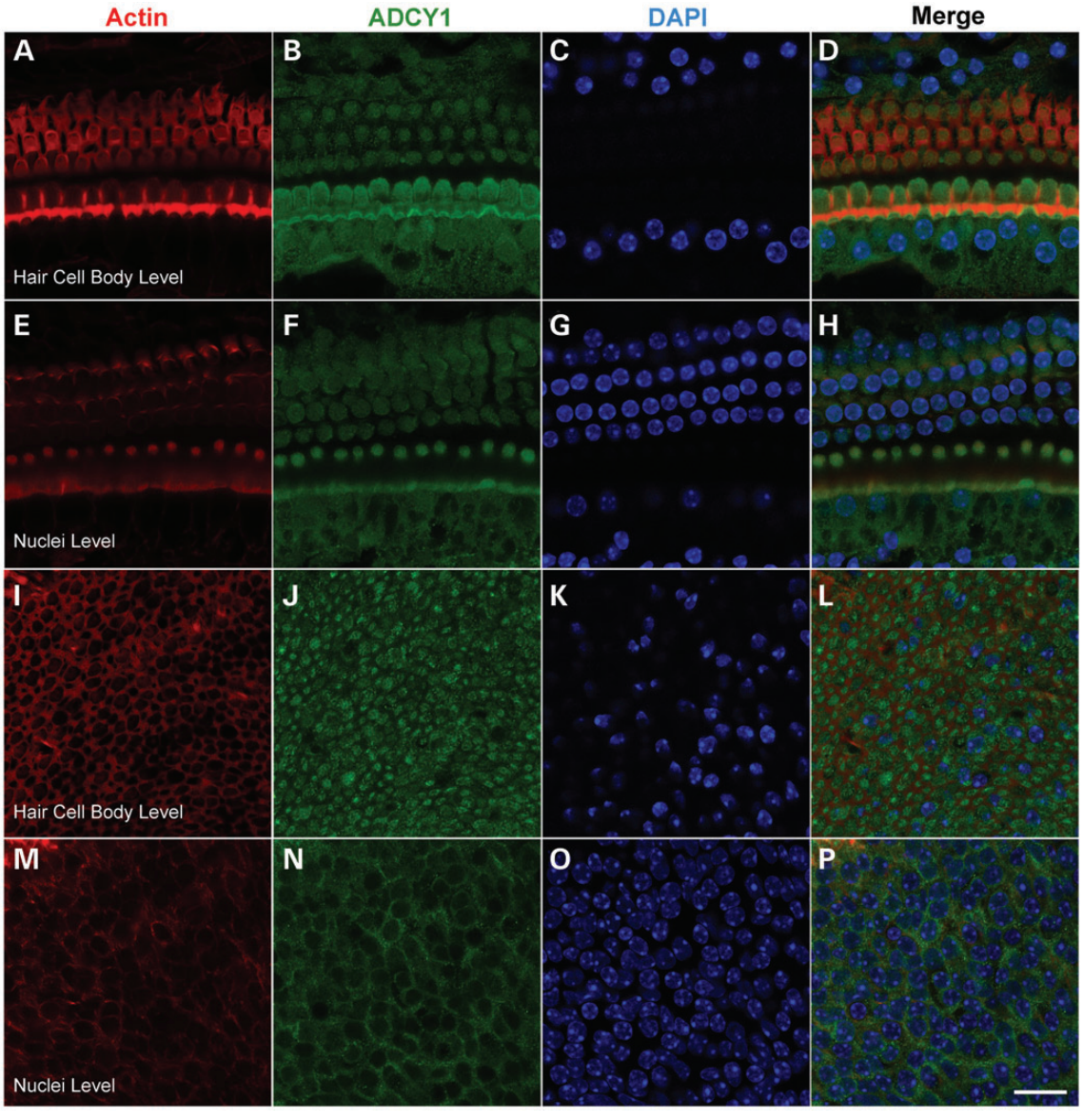

Figure 3. ADCY1 localization to sensory epithelium in mouse inner ear. (**A**)–(**H**) show immunostaining in cochlear hair cells, while (**I**)–(**P**) show labeling of vestibular hair cells. (A–D) and (I–L) were taken at the level of hair cell bodies, while panels (E–H) and (M–P) were taken at the nuclei level. Specifically (I)–(L) show staining at hair cell body level under the cuticular plate. Scale bar in (P) is 10 μm and applies to all panels. Actin cytoskeleton of the organ of Corti and vestibular sensory epithelia cells is highlighted by rhodamine-phalloidin (red) in (A), (E), (I) and (M). ADCY1 localization is highlighted in green in (B), (F), (J) and (N). DAPI was used as nuclei marker (blue) in (C), (G), (K) and (O). Rightmost panels (D), (H), (L) and (P) represent merged images. ADCY1 is localized to cochlear outer and inner hair cell bodies and nuclei (B, D, F, H). Barely detectable level of ADCY1 was observed in the hair cell stereocilia (data not shown). Supporting cells around outer hair cells have weaker staining by anti-ADCY1 antibody than hair cells. ADCY1 localizes to the vestibular hair cell bodies and also in supporting cells (green), but no nuclei labeling was observed (J, L, N, P).

resolution immunofluorescent labeling, these results support the conclusion that ADCY1 localizes to actin-based microvilli and stereocilia (Fig. 4 and A), but truncation of the carboxyl tail can prevent its normal localization and potentially affect its function in the stereocilia.

DISCUSSION

Due to the haplotypes in Branch 2 of family 4009, it was not initially clear whether this branch of the family segregated the same causal variant as Branch 1. Within the DFNB44 region, for branch 1 all hearing-impaired individuals are homozygous for STR markers D7S2846 and D7S1818, while for branch 2 hearing-impaired individual V-9 is heterozygous for both of these markers (Fig. 1A). This observation could have been due to (i) incorrect phenotype information, (ii) locus heterogeneity, i.e. branches 1 and 2 segregate different causal variants, or (iii) due to the large physical distances between the STR markers. After performing WES, it became clear that the two branches of the family segregated the same variant and that the lack of observation of homozygosity for the STR markers was due to the

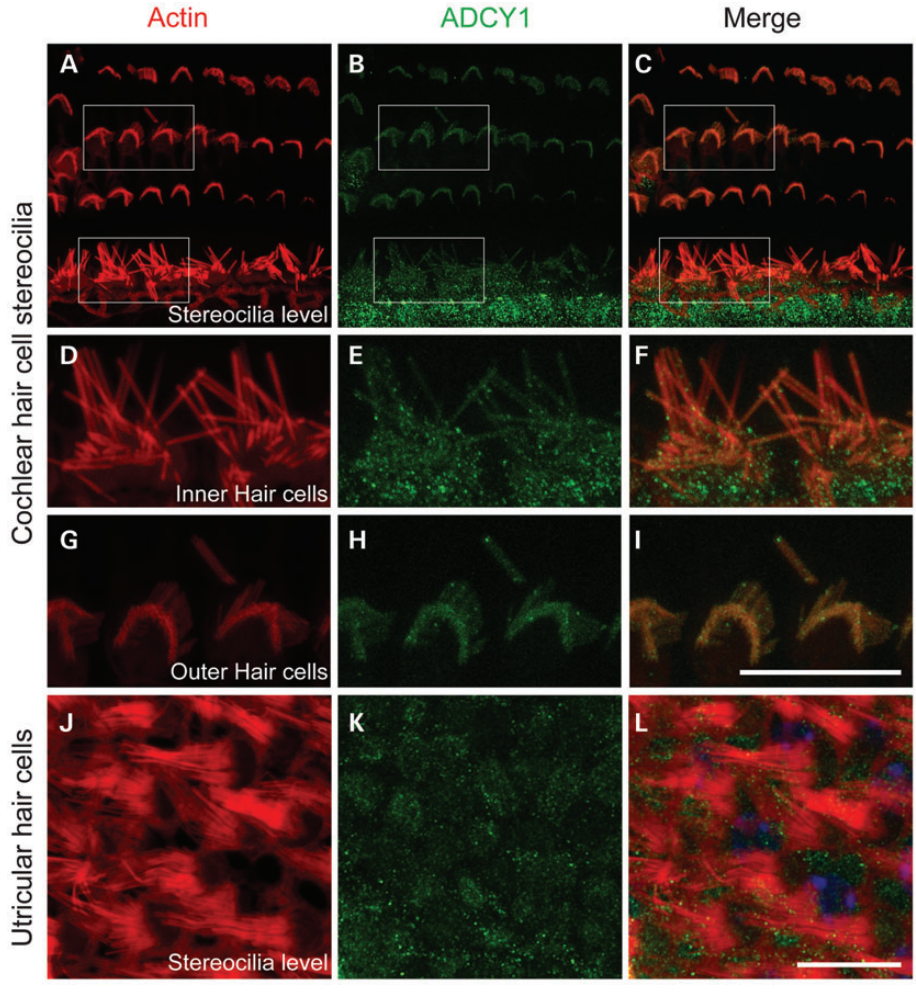

Figure 4. ADCY1 localization to rat cochlear hair cell stereocilia. (**A**)–(**I**) show immunostaining in cochlear hair cells, while (**J**)–(**L**) show labeling of utricular hair cells. Scale bars in (I) and (L) are 10 μm. Boxed regions in (A)–(C) are magnified in (D) to (I). Actin cytoskeleton of the organ of Corti and vestibular sensory epithelial cells is highlighted by rhodamine-phalloidin (red) in (A), (D), (G) and (J). ADCY1 localization is highlighted in green (B, E, H, K). Rightmost panels (C, F, I, L) represent merged images. ADCY1 is localized to the adult rat inner hair cell bodies and stereocilia of both inner and outer hair cells (B–C, E–F, H-I). Anti-ADCY1 labeling was observed along the length of stereocilia. Similar to the mouse, anti-ADCY1 labeling was observed in cell bodies of utricular hair cells in the adult rat vestibule, but no ADCY1 localization was observed in hair cell bundles (K–L).

large physical distance between these markers. Individuals VI-3 and V-9 share a 3.84 Mb region (Supplementary Material, Table S2) which lies between STR markers D7S2846 and D7S1818. Although it was reported that the two branches of family 4009 are only related by marriage, given that they share the same rare *ADCY1* variant, they must also be biologically related. Additionally after gene identification, we were able to obtain audiograms for individuals from both branches of the pedigree and they present with similar phenotypes. The sharing of this unusual hearing impairment phenotype also provides supportive evidence that the two branches are biologically related.

ACs catalyze the conversion of adenosine triphosphate (ATP) to pyrophosphate and the second-messenger cyclic AMP (cAMP), which regulates signal transduction in the inner ear, e.g. during MET or the conversion of mechanical energy (i.e. fluid movement within the cochlear duct due to sound or within the semicircular canal due to head motion) into neural impulses by the hair cells (16,17). Selective exposure of hair cell plasma membranes to increased cAMP levels results in increased membrane conductance (18). Within the hair cell membrane, at least two ion channels that are primarily activated by cAMP have been identified, namely cyclic nucleotide-sensitive channel HCN1 (19), which produces a slow, inward K^+-Na^+ current after hyperpolarization, and is directly bound to protocadherin 15 at stereociliary tip-links (20); and the voltage-gated channel KCNQ4, which produces a slow, activating outward K^+ current that is enhanced by cAMP (21), and in which genetic variation causes autosomal dominant hearing loss (22). There is also evidence that in avian ear, regenerative proliferation of hair cells is regulated by cAMP (23).

Despite the importance of cAMP production in hair cells, knowledge of the role of AC within the hair cell is limited. Of the nine transmembrane AC genes, AC 1, 5, 6 and 9 are known to be expressed within hair cells (24, 25). Most of the past studies on AC function within the inner ear were not gene- or protein-specific and were thus focused not on the hair cell but on the stria vascularis, where aggregate expression of

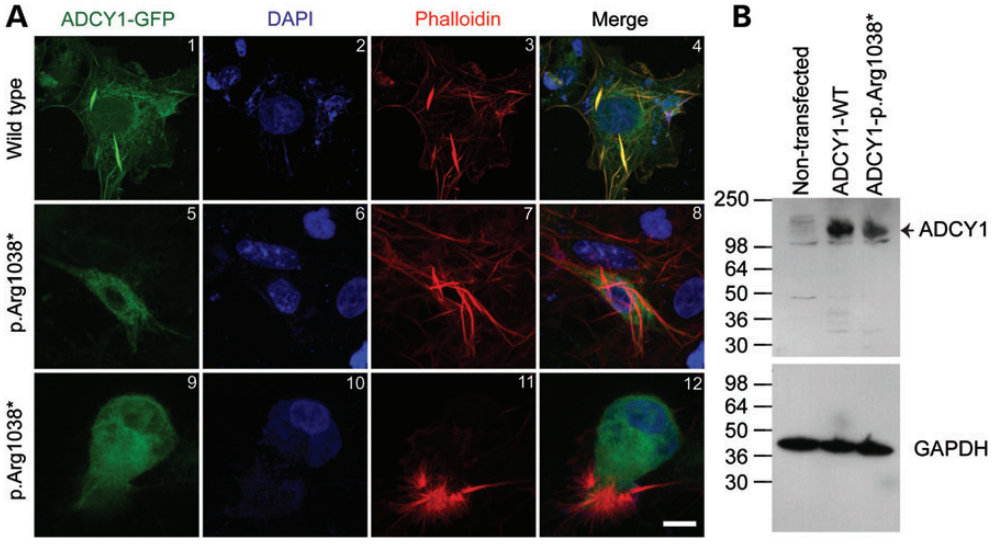

Figure 5. ADCY1 accumulation at actin-based structures. (**A**) The localization of wild-type and mutant ADCY1 using espin-mediated microvillar elongation. COS-7 cells were co-transfected with GFP-tagged ADCY1 (green, panels 1, 5 and 9) and untagged espin constructs (Supplementary Material, Fig. S4C). DAPI was used as nuclei marker (blue, panels 2, 6 and 10). Rhodamine-phalloidin (red, panels 3, 7 and 11) was used to reveal F-actin and highlight the microvilli on the COS-7 cell surface. Rightmost panels (4, 8 and 12) represent merged images. Panels 1–8 show the apical cell surface, while panels 9–12 show the basal surface. Scale bar in panel 12: 10 μm. Wild-type ADCY1 (panels 1 and 4) was efficiently targeted to the microvillar actin bundles at the cell surface. ADCY1 with the p.Arg1038* variant (panels 5 and 8, apical surface; panels 9 and 12, basal surface) had no microvillar or cell membrane targeting and remained in the cytoplasm. (**B**) Western blot analysis of GFP-tagged wild-type and p.Arg1038* mutant protein expressed in COS-7 cells. GAPDH was used as a loading control. No statistically significant difference in normalized amounts was seen between wild-type and mutant protein.

AC genes is highest but is mostly due to *Adcy2* (26). Previous studies using immunohistochemistry on paraffin-embedded organ of Corti revealed weak ADCY1 immunoreactivity in the outer hair cells, stria vascularis and spiral ligament, while strong staining was seen in auditory nerve, supporting cells and to both the cell body and stereocilia of inner hair cells (24,27). In this study, ADCY1 was localized to the cytoplasm of supporting cells and hair cells of the cochlea and vestibule and also to cochlear hair cell nuclei and stereocilia.

The ADCY1 p.Arg1038* variant is predicted to result in the loss of two β sheets β7′–β8′ within the C_2 domain (Fig. 1C), which includes highly conserved residues particularly amino acids at positions 1037–1053 (Supplementary Material, Fig. S2). When the sequence of rat ADCY2 is aligned with that of human ADCY1, the lysine residue at position 1044 of human ADCY1 aligns with p.Lys1065 from rat ADCY2 and is shown to be identical in all human transmembrane AC proteins and similar proteins across species (Fig. 1D, Supplementary Material, Fig. S2). Previous crystallographic studies have shown that the p.Lys1065 residue lies within the AC catalytic domain and is predicted to participate in ATP binding (28). MutationTaster also predicts the loss of a calmodulin (CaM)-interacting site due to the p.Arg1038* variant. Moreover in COS-7 cells, truncated ADCY1 did not localize properly to microvilli, suggesting that conserved elements within the carboxyl tail not only participate in catalysis but are also essential for membrane targeting. Based on these results, the ADCY1 p.Arg1038* variant is predicted to diminish cAMP production within hair cells, particularly in stereocilia.

Localization of ADCY1 to stereocilia suggests its involvement in the regulation of MET channels in hair cells through cAMP production. Hair cell stereocilia are connected by tip-links, which are thought to be directly connected to MET channels. The tip-links open or close MET channels when the direction of deflection of stereocilia is toward or away from the tallest row of stereocilia. Recently, it was proposed that two different channel proteins are each connected at either end of the tip-link, with HCN1 at the top of the shorter stereocilium and CNGA3 at the lateral position of the taller stereocilium within the staircase-like structure of the stereociliary array (29). Interestingly, both HCN1 and CNGA3 are stimulated by cAMP (30,31). Modulation of MET channel activity by ADCY1 through cAMP production is further supported by failure of FM1-43 dye uptake in *adcy1b* morphant zebrafish. The *adcy1b* morphant zebrafish were also demonstrated to have gross hearing defects, which establishes the importance of *ADCY1* to hair cells in the inner ear.

Although AC proteins are well described in the literature, the deleterious effect of AC gene variation on *in vivo* auditory function has not been reported previously. One article on *Adcy1*-mutant mice mentioned no functional loss in short- and long-latency auditory evoked responses (32), which may not be reliable for hearing threshold measurement particularly for moderate cochlear loss (33). The $Adcy1^{-/-}$ mouse has been studied for multiple neurologic phenotypes including poor spatial memory (34), reduced opiate withdrawal (35) and less response to injury-mediated inflammatory pain (36). Although mapping changes in higher-order neurons were documented in *Adcy1*-mutant mice (37,38), gross motor, balance or visual deficits were not established (32,34,36). It should be noted that within family 4009, aside from hearing impairment, no other neurologic or vestibular phenotypes were identified. In addition, the neurologic phenotypes that were identified in $Adcy1^{-/-}$ mice are very difficult to detect in humans by standard clinical testing, e.g. spatial memory, opiate withdrawal.

Hearing-impaired members of family 4009 had predominantly mixed hearing impairment that was on average moderate in

severity. This might seem to contradict the gross hearing defect that is seen in *adcy1b* morphant zebrafish, but it is plausible that hearing loss severity might depend on the affected protein domain. In a previous enzymatic assay, truncation of ADCY1 at the C_{2b} subdomain decreased but did not abolish catalytic function (39). Note that for *adcy1b* morphant zebrafish with gross hearing defects, protein truncation occurs at the C_1 domain (12), and therefore a larger segment of the protein is removed. Another possibility why mutated ADCY1 has a moderate effect on hearing is complementation among different AC proteins. Eight AC genes are expressed in the inner ear, and expression within the organ of Corti is highest for *ADCY9* while low-level expression was detected for other AC genes including *ADCY1* (26). Previous hair-cell-specific studies demonstrated labeling of AC 1, 5, 6 and 9 in stereocilia (24,25). Among the AC proteins, ADCY1 is most similar in sequence to ADCY5 and ADCY6 (Supplementary Material, Fig. S2B), but there are differences in their pattern of distribution. For example, ADCY6 labeling is restricted to the stereociliary base at P3 onward (25), while ADCY1 is found along the length of stereocilia throughout inner ear development and maturation, with highest levels found at P16. The expression of these proteins within hair cells but at different developmental stages and localization suggests protein-specific roles within the hair cell and stereocilia.

In summary, our results strongly support a role of ADCY1 in the regulation of MET channel activity within hair cell stereocilia. So far, a rare variant in only one AC gene, *ADCY5* (MIM 600293), causes autosomal dominant familial dyskinesia with facial myokymia (40). The hypothesis that an *ADCY1* mutation can cause hearing impairment through defects in signal transduction within the hair cell is consistent with the concept of neurologic phenotypes due to rare AC variants. Loss of ADCY1 function causes hearing impairment in both humans and zebrafish, which clearly supports the importance of cAMP signaling via ADCY1 to hair cell function within the inner ear.

MATERIALS AND METHODS

The study was approved by the Institutional Review Boards of Quaid-i-Azam University and Baylor College of Medicine and Affiliated Hospitals. Informed consent was obtained from all family members who participated in the study. Multiple family members were interviewed for familial history of hearing impairment and pedigree relations. Physical examinations were performed on all participating family members. Hearing impairment was verified in six of the eight individuals who are homozygous for the *ADCY1* mutation through standard audiometric testing (Fig. 1A and B; Supplementary Material, Fig. S1).

DNA samples of hearing-impaired individuals VI-3 and V-9 (Fig. 1A) were submitted for WES at the University of Washington Center for Mendelian Genomics. For individual VI-3, sequence capture was performed in solution with the Roche NimbleGen SeqCap EZ Human Exome Library v2.0 (~36.6 Mb of target sequence), while for individual V-9 the NimbleGen Big Exome 2011 Library (EZ Exome v3.0 with ~64 Mb target sequence) was used. Sequencing was performed using an Illumina HiSeq to average read depth of 112× for sample VI-3 and 61× for sample V-9. Fastq files were aligned to the hg19 human reference sequence using Burrows-Wheeler Aligner (BWA) (http://bio-bwa.sourceforge.net/; 41). Realignment of regions containing indels, recalibration of base qualities, and variant detection and calling were performed using the Genome Analysis Toolkit (GATK) (http://www.broadinstitute.org/gatk/; 42). Variant sites that are of low quality and more likely to be false-positives were flagged. Annotation of variant sites was performed using SeattleSeq 137 (http://snp.gs.washington.edu/SeattleSeqAnnotation137/).

DNA samples from 17 members of family 4009, including 8 hearing-impaired and 9 unaffected individuals, were submitted to a genome scan at the Center for Inherited Disease Research using 388 fluorescently labeled STR markers. Two-point linkage analysis using genotypes for the *ADCY1* stop-gained variant and STR markers was performed with Superlink (43). Haplotypes were reconstructed using three different programs, namely SimWalk v2.91 (44), Allegro 2.0 (45) and MERLIN (46).

To determine the evolutionary conservation of the ADCY1 segment that is removed by the nonsense variant p.Arg1038*, sequences similar to human ADCY1 were derived from the UniProt database (http://www.uniprot.org) for 52 animal species, including 6 primates, 20 other mammals, 2 birds, 2 reptiles, 1 amphibian, 6 bony fish, 9 insects, 2 arthropods, 2 mollusks, lancelet and trichoplax (Supplementary Material, Fig. S2A). These 52 protein sequences and the sequences of 8 human transmembrane AC proteins (Supplementary Material, Fig. S2) were aligned with human ADCY1 using Clustal Omega (http://www.ebi.ac.uk/Tools/msa/clustalo/; 47). To further investigate putative changes to structure and function due to the stop-gained variant, the secondary structures of wild-type and truncated ADCY1 were compared using predicted structures from SWISS-MODEL (http://swissmodel.expasy.org/; 48) based on the C_{2a} subdomain of rat ADCY2 (Protein Data Bank ID 1CUL; 49).

All animals used in this study were kept with the approval of the Institutional Animal Care and Use Committee of the Cincinnati Children's Research Foundation. In order to generate gene copy-specific morphants, we used previously validated splice-site blocking morpholinos that induce altered splicing and protein truncation within the C_1 domain (12). The morpholinos were micro-injected at one- to two-cell stage and the resulting embryos were phenotyped at 72 h post-fertilization (Fig. 2A, Supplementary Material, Fig. S3). To investigate hearing function, we measured the startle response in both *adcy1a* and *adcy1b* 5-day-old morphants by tapping on the dish. To assess the functional status of neuromast hair cells in the lateral lines of zebrafish, we briefly exposed the wild-type, *adcy1a* and *adcy1b* larvae to FM1-43 dye.

In order to determine the relative expression of *Adcy1* (NM_009622) in mouse inner ear, real-time PCR was performed using *Adcy1*-specific primers and cDNA libraries prepared from mouse temporal bones at various developmental stages (Fig. 2C). The data were normalized against *Gapdh* (NM_008084) as an internal control (ΔCt) and were further normalized against *Adcy1* expression at P3 developmental stage (ΔΔCt). To determine the localization of ADCY1 at high resolution in the organ of Corti of the mouse and rat, we performed immunofluorescence using commercially available anti-ADCY1 antibodies (Biorbyt LLC, San Francisco, CA, USA) and imaging by confocal microscopy. Western blot analysis of anti-ADCY1 antibody on protein extract from P17 C57BL/6 mouse inner ear homogenate (50 μg/lane) showed a band corresponding to the predicted protein size for mouse ADCY1 (~123 kDa; Supplementary Material, Fig. S4A).

The anti-serum to ADCY1 was further validated in heterologous cells (Supplementary Material, Fig. S4B). The immunolocalization of ADCY1 was then examined in the adult organ of Corti and vestibular sensory epithelium.

We also examined COS-7 cells to understand the mechanism and effect of ADCY1 with the p.Arg1038* variant. We transiently co-transfected GFP-tagged human *ADCY1* constructs (Fig. 5A) and a construct to induce the expression of non-tagged *ESPN* (NM_031475.2) at the cell surface to over-elongate the microvilli (50; Supplementary Material, Fig. S4C).

SUPPLEMENTARY MATERIAL

Supplementary Material is available at *HMG* online.

ACKNOWLEDGEMENTS

We are very grateful to family members who participated in the study.

Conflict of Interest statement. None declared.

FUNDING

This work was funded by: the National Institutes of Health (NIH)—National Institute on Deafness and Other Communication Disorders (grant numbers R01 DC003594, R01 DC011651 to S.M.L.; and R01 DC011803, R01 DC012564 to S.R. and Z.M.A .); the NIH—National Human Genome Research Institute and NIH—National Heart, Lung, and Blood Institute (grant U54 HG006493 to the University of Washington Center for Mendelian Genomics); and the Higher Education Commission, Government of Pakistan (to W.A.). Genotyping was performed at the Center for Inherited Disease Research, which is funded by the NIH (contract number N01 HG65403 to the Johns Hopkins University).

REFERENCES

1. Yaeger, D., McCallum, J., Lewis, K., Soslow, L., Shah, U., Potsic, W., Stolle, C. and Krantz, I.D. (2006) Outcomes of clinical examination and genetic testing of 500 individuals with hearing loss evaluated through a genetics of hearing loss clinic. *Am. J. Med. Genet. A*, **140**, 827–836.
2. Ansar, M., Chahrour, M.H., Amin ud Din, M., Arshad, M., Haque, S., Pham, T.L., Yan, K., Ahmad, W. and Leal, S.M. (2004) DFNB44, a novel autosomal recessive non-syndromic hearing impairment locus, maps to chromosome 7p14.1-q11.22. *Hum. Hered.*, **57**, 195–199.
3. Adzhubei, I.A., Schmidt, S., Peshkin, L., Ramensky, V.E., Gerasimova, A., Bork, P., Kondrashov, A.S. and Sunyaev, S.R. (2010) A method and server for predicting damaging missense mutations. *Nat. Methods*, **7**, 248–249.
4. Choi, Y., Sims, G.E., Murphy, S., Miller, J.R. and Chan, A.P. (2012) Predicting the functional effect of amino acid substitutions and indels. *PLoS ONE*, **7**, e46688.
5. Ng, P.C. and Henikoff, S. (2001) Predicting deleterious amino acid substitutions. *Genome Res.*, **11**, 863–874.
6. Schwarz, J.M., Rodelsperger, C., Schuelke, M. and Seelow, D. (2010) MutationTaster evaluates disease-causing potential of sequence alterations. *Nat. Methods*, **7**, 575–576.
7. Reva, B., Antipin, Y. and Sander, C. (2011) Predicting the functional impact of protein mutations: applications to cancer genomics. *Nucleic Acids Res.*, **39**, e118.
8. Chun, S. and Fay, J.C. (2009) Identification of deleterious mutations within three human genomes. *Genome Res.*, **19**, 1553–1561.
9. Shihab, H.A., Gough, J., Cooper, D.N., Stenson, P.D., Barker, G.L.A., Edwards, K.J., Day, I.N.M. and Gaunt, T.R. (2013) Predicting the functional, molecular and phenotypic consequences of amino acid substitutions using hidden Markov models. *Hum. Mutat.*, **34**, 57–65.
10. Nicolson, T. (2005) The genetics of hearing and balance in zebrafish. *Annu. Rev. Genet.*, **39**, 9–22.
11. Riazuddin, S., Belyantseva, I.A., Giese, A.P., Lee, K., Indzhykulian, A.A., Nandamuri, S.P., Yousaf, R., Sinha, G.P., Lee, S., Terrell, D. *et al.* (2012) Alterations of CIB2 calcium- and integrin-binding protein cause Usher syndrome type 1J and nonsyndromic deafness DFNB48. *Nat. Genet.*, **44**, 1265–1271.
12. Xu, H., Leinwand, S.G., Dell, A.L., Fried-Cassorla, E. and Raper, J.A. (2010) The calmodulin-stimulated adenylate cyclase ADCY8 sets the sensitivity of zebrafish retinal axons to midline repellents and is required for normal midline crossing. *J. Neurosci.*, **30**, 7423–7433.
13. Gale, J.E., Marcotti, W., Kennedy, H.J., Kros, C.J. and Richardson, G.P. (2001) FM1–43 dye behaves as a permeant blocker of the hair-cell mechanotransducer channel. *J. Neurosci.*, **21**, 7013–7025.
14. Rzadzinska, A.K., Schneider, M.E., Davies, C., Riordan, G.P. and Kachar, B. (2004) An actin molecular treadmill and myosins maintain stereocilia functional architecture and self-renewal. *J. Cell Biol.*, **164**, 887–897.
15. Perrot-Applanat, M., Lescop, P. and Milgrom, E. (1992) The cytoskeleton and cellular traffic of the progesterone receptor. *J. Cell Biol.*, **119**, 337–348.
16. Ricci, A.J. and Fettiplace, R. (1997) The effects of calcium buffering and cyclic AMP on mechano-electrical transduction in turtle auditory hair cells. *J. Physiol.*, **501**, 111–124.
17. Kimitsuki, T., Matsuda, K. and Komune, S. (2006) Calcium action on the membrane currents possessing the properties of mechano-electric transducer currents in inner hair cells of the guinea-pig cochlea. *Int. J. Neurosci.*, **116**, 1327–1335.
18. Kolesnikov, S.S., Rebrik, T.I., Zhainazarov, A.B., Tavartkiladze, G.A. and Kalamkarov, G.R. (1991) A cyclic-AMP-gated conductance in cochlear hair cells. *FEBS Lett.*, **290**, 167–170.
19. Cho, W.J., Drescher, M.J., Hatfield, J.S., Bessert, D.A., Skoff, R.P. and Drescher, D.G. (2003) Hyperpolarization-activated, cyclic AMP-gated, HCN1-like cation channel: the primary full-length HCN isoform expressed in a saccular hair-cell layer. *Neuroscience*, **118**, 525–534.
20. Ramakrishnan, N.A., Drescher, M.J., Khan, K.M., Hatfield, J.S. and Drescher, D.G. (2012) HCN1 and HCN2 proteins are expressed in cochlear hair cells: HCN1 can form a ternary complex with protocadherin 15 CD3 and F-actin-binding filamin A or can interact with HCN2. *J. Biol. Chem.*, **287**, 37628–37646.
21. Chambard, J.M. and Ashmore, J.F. (2005) Regulation of the voltage-gated potassium channel KCNQ4 in the auditory pathway. *Pflugers Arch.*, **450**, 34–44.
22. Kubisch, C., Schroeder, B.C., Friedrich, T., Lütjohann, B., El-Amraoui, A., Marlin, S., Petit, C. and Jentsch, T.J. (1999) KCNQ4, a novel potassium channel expressed in sensory outer hair cells, is mutated in dominant deafness. *Cell*, **96**, 437–446.
23. Navaratnam, D.S., Su, H.S., Scott, S.P. and Oberholtzer, J.C. (1996) Proliferation in the auditory receptor epithelium mediated by a cyclic AMP-dependent signaling pathway. *Nat. Med.*, **2**, 1136–1139.
24. Drescher, M.J., Khan, K.M., Beisel, K.W., Karadaghy, A.A., Hatfield, J.S., Kim, S.Y., Drescher, A.J., Lasak, J.M., Barretto, R.L., Shajir, A.H. *et al.* (1997) Expression of adenylyl cyclase type I in cochlear inner hair cells. *Brain Res. Mol. Brain Res.*, **45**, 325–330.
25. Michalski, N., Michel, V., Bahloul, A., Lefèvre, G., Barral, J., Yagi, H., Chardenoux, S., Weil, D., Martin, P., Hardelin, J.P. *et al.* (2007) Molecular characterization of the ankle-link complex in cochlear hair cells and its role in the hair bundle functioning. *J. Neurosci.*, **27**, 6478–6488.
26. Kumagami, H., Beitz, E., Wild, K., Zenner, H.P., Ruppersberg, J.P. and Schultz, J.E. (1999) Expression pattern of adenylyl cyclase isoforms in the inner ear of the rat by RT-PCR and immunochemical localization of calcineurin in the organ of Corti. *Hear Res.*, **132**, 69–75.
27. Drescher, M.J., Khan, K.M., Hatfield, J.S., Shakir, A.H. and Drescher, D.G. (2000) Immunohistochemical localization of adenylyl cyclase isoforms in the lateral wall of the rat cochlea. *Brain Res. Mol. Brain Res.*, **76**, 289–298.
28. Tesmer, J.J., Sunahara, R.K., Gilman, A.G. and Sprang, S.R. (1997) Crystal structure of the catalytic domains of adenylyl cyclase in a complex with Gsalpha.GTPgammaS. *Science*, **278**, 1907–1916.
29. Selvakumar, D., Drescher, M.J. and Drescher, D.G. (2013) Cyclic nucleotide-gated channel α-3 (CNGA3) interacts with stereocilia tip-link

cadherin 23 + exon 68 or alternatively myosin VIIa, two proteins required for hair cell mechanotransduction. *J. Biol. Chem.*, **288**, 7215–7229.
30. Wainger, B.J., DeGennaro, M., Santoro, B., Siegelbaum, S.A. and Tibbs, G.R. (2001) Molecular mechanism of cAMP modulation of HCN pacemaker channels. *Nature*, **411**, 805–810.
31. Gerstner, A., Zong, X., Hofmann, F. and Biel, M. (2000) Molecular cloning and functional characterization of a new modulatory cyclic nucleotide-gated channel subunit from mouse retina. *J. Neurosci.*, **20**, 1324–1332.
32. Tremblay, F., Abdel-Majid, R. and Neumann, P.E. (2002) Electroretinographic oscillatory potentials are reduced in adenylyl cyclase type I deficient mice. *Vision Res.*, **42**, 1715–17225.
33. Beattie, R.C., Garcia, E. and Johnson, A. (1996) Frequency-specific auditory brainstem responses in adults with sensorineural hearing loss. *Audiology*, **35**, 194–203.
34. Wu, Z.L., Thomas, S.A., Villacres, E.C., Xia, Z., Simmons, M.L., Chavkin, C., Palmiter, R.D. and Storm, D.R. (1995) Altered behavior and long-term potentiation in type I adenylyl cyclase mutant mice. *Proc. Natl Acad. Sci. USA*, **92**, 220–224.
35. Zachariou, V., Liu, R., LaPlant, Q., Xiao, G., Renthal, W., Chan, G.C., Storm, D.R., Aghajanian, G. and Nestler, E.J. (2008) Distinct roles of adenylyl cyclases 1 and 8 in opiate dependence: behavioral, electrophysiological, and molecular studies. *Biol. Psychiatry*, **63**, 1013–1021.
36. Vadakkan, K.I., Wang, H., Ko, S.W., Zastepa, E., Petrovic, M.J., Sluka, K.A. and Zhuo, M. (2006) Genetic reduction of chronic muscle pain in mice lacking calcium/calmodulin-stimulated adenylyl cyclases. *Mol. Pain*, **2**, 7.
37. Welker, E., Armstrong-James, M., Bronchti, G., Ourednik, W., Gheorghita-Baechler, F., Dubois, R., Guernsey, D.L., Van der Loos, H. and Neumann, P.E. (1996) Altered sensory processing in the somatosensory cortez of the mouse mutant barrelless. *Science*, **271**, 1864–1867.
38. Ravary, A., Muzerelle, A., Hervé, D., Pascoli, V., Ba-Charvet, K.N., Girault, J.A., Welker, E. and Gaspar, P. (2003) Adenylate cyclase 1 as a key factor in the refinement of retinal projection maps. *J. Neurosci.*, **23**, 2228–2238.
39. Diel, S., Beyermann, M., Lloréns, J.M., Wittig, B. and Kleuss, C. (2008) Two interaction sites on mammalian adenylyl cyclase type I and II: modulation by calmodulin and G(betagamma). *Biochem. J.*, **411**, 449–456.
40. Chen, Y.Z., Matsushita, M.M., Robertson, P., Rieder, M., Girirajan, S., Antonacci, F., Lipe, H., Eichler, E.E., Nickerson, D.A., Bird, T.D. *et al.* (2012) Autosomal dominant familial dyskinesia and facial myokymia: single exome sequencing identifies a mutation in adenylyl cyclase 5. *Arch. Neurol.*, **69**, 630–635.
41. Li, H. and Durbin, R. (2009) Fast and accurate short read alignment with Burrows-Wheeler transform. *Bioinformatics*, **25**, 1754–1760.
42. McKenna, A., Hanna, M., Banks, E., Sivachenko, A., Cibulskis, K., Kernytsky, A., Garimella, K., Altshuler, D., Gabriel, S., Daly, M. *et al.* (2010) The genome analysis toolkit: a MapReduce framework for analyzing next-generation DNA sequencing data. *Genome Res.*, **20**, 1297–1303.
43. Fishelson, M. and Geiger, D. (2002) Exact genetic linkage computations for general pedigrees. *Bioinformatics*, **18**, S189–S198.
44. Sobel, E. and Lange, K. (1996) Descent graphs in pedigree analysis: applications to haplotyping, location scores and marker sharing statistics. *Am. J. Hum. Genet.*, **58**, 1323–1337.
45. Gudbjartsson, D.F., Thorvaldsson, T., Kong, A., Gunnarsson, G. and Ingolfsdottir, A. (2005) Allegro version 2. *Nat. Genet.*, **37**, 1015–1016.
46. Abecasis, G.R., Cherny, S.S., Cookson, W.O. and Cardon, L.R. (2002) Merlin—rapid analysis of dense genetic maps using sparse gene flow trees. *Nat. Genet.*, **30**, 97–101.
47. Sievers, F., Wilm, A., Dineen, D., Gibson, T.J., Karplus, K., Li, W., Lopez, R., McWilliam, H., Remmert, M., Söding, J. *et al.* (2011) Fast, scalable generation of high-quality protein multiple sequence alignment using Clustal Omega. *Mol. Syst. Biol.*, **7**, 539.
48. Arnold, K., Bordoli, L., Kopp, J. and Schwede, T. (2006) The SWISS-MODEL workspace: a web-based environment for protein structure homology modelling. *Bioinformatics*, **22**, 195–201.
49. Tesmer, J.J., Dessauer, C.W., Sunahara, R.K., Murray, L.D., Johnson, R.A., Gilman, A.G. and Sprang, S.R. (2000) Molecular basis for P-site inhibition of adenylyl cyclase. *Biochemistry*, **39**, 14464–14471.
50. Loomis, P.A., Zheng, L., Sekerková, G., Changyaleket, B., Mugnaini, E. and Bartles, J.R. (2003) Espin cross-links cause the elongation of microvillus-type parallel actin bundles in vivo. *J. Cell Biol.*, **163**, 1045–1055.